Supporting Information

Lithiation of multilayer Ni/NiO conversion electrodes:

Criticality of nickel layer thicknesses on conversion reaction kinetics

Guennadi Evmenenko,[a] Timothy T. Fister,[b] D. Bruce Buchholz,[a] Fernando C. Castro,[c] Qianqian Li,[c] Jinsong Wu,[a,c] Vinayak P. Dravid,[a] Paul Fenter,[b] Michael J. Bedzyk[a,d]

[a] *Department of Materials Science and Engineering, Northwestern University, Evanston, Illinois 60208, United States*

[b] *Chemical Sciences and Engineering Division, Argonne National Laboratory, Lemont, Illinois 60439, United States*

[c] *EPIC, NUANCE Center, Northwestern University, Evanston, Illinois 60208, United States*

[d] *Department of Physics and Astronomy, Northwestern University, Evanston, Illinois 60208, USA*

Details of multilayer film growth. Nickel - nickel oxide multilayer thin-films were grown by pulsed-laser deposition (PLD) using a 248 nm KrF excimer laser with a 25 ns pulse duration and operated at 2 Hz. The laser pulse was focused onto a 1.5 mm x 2.5 mm spot size. Nickel was deposited from a metallic nickel target at an energy of 300 mJ per pulse without the introduction of a reactant gas after the chamber had pumped down to a base pressure of ~5×10^{-7} Torr. Nickel oxide was deposited from a dense hot-pressed nickel oxide target at an energy of 200 mJ per pulse in a deposition ambient of 5×10^{-4} Torr UHP oxygen. The targets were rotated at 5-rpm about their axis to prevent localized heating. The target-substrate separation was fixed at 10 cm. The thickness of each layer was controlled by adjusting the number of laser pulses.

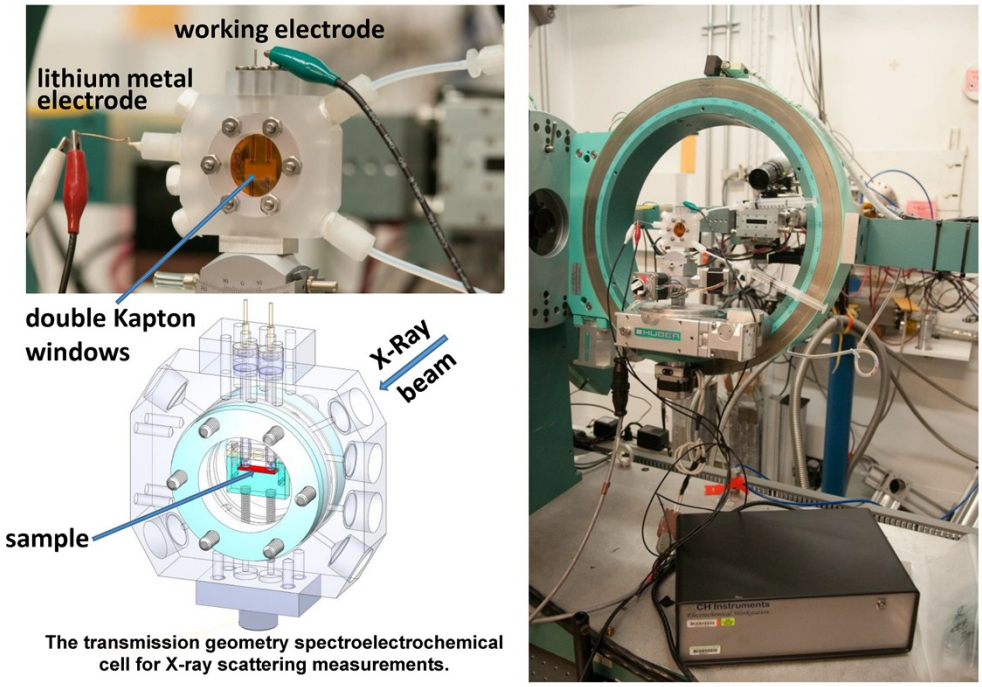

The transmission geometry spectroelectrochemical cell used to measure X-ray reflectivity and in-operando X-ray experimental setup at APS.

Table S1. Tablulated mass densities (ρ) and calculated electron densities (ρ_e) of assumed components of the Ni/NiO multilayer electrode.

Compound	Density ρ (g/cm^3)	Electron density at 17.5 keV ρ_e (e$^-$Å^{-3})*	Electron density at 8.04 keV ρ_e (e$^-$Å^{-3})*
1 M $LiPF_6$ EC/DMC (1:1 v/v)	1.2	0.38	0.38
NiO	6.67	1.97	1.78
Ni	8.90	2.60	2.28
Li_2O	2.01	0.57	0.57
sapphire	3.97	1.18	1.19

*The electron density, ρ_e, of each layer was calculated from the atomic composition of the compound according to the relationship: $\rho_e = \sum_i (Z_i - \Delta f_i) \cdot \rho \cdot N_A / M$. Here Z_i is the number of electrons in the i^{th} atom, Δf_i is the anomalous dispersion correction. The summation is carried out over all atoms in the molecular formula for the compound. N_A is Avogadro's number, M is the molecular mass of the compound, and ρ is the mass density of the compound.

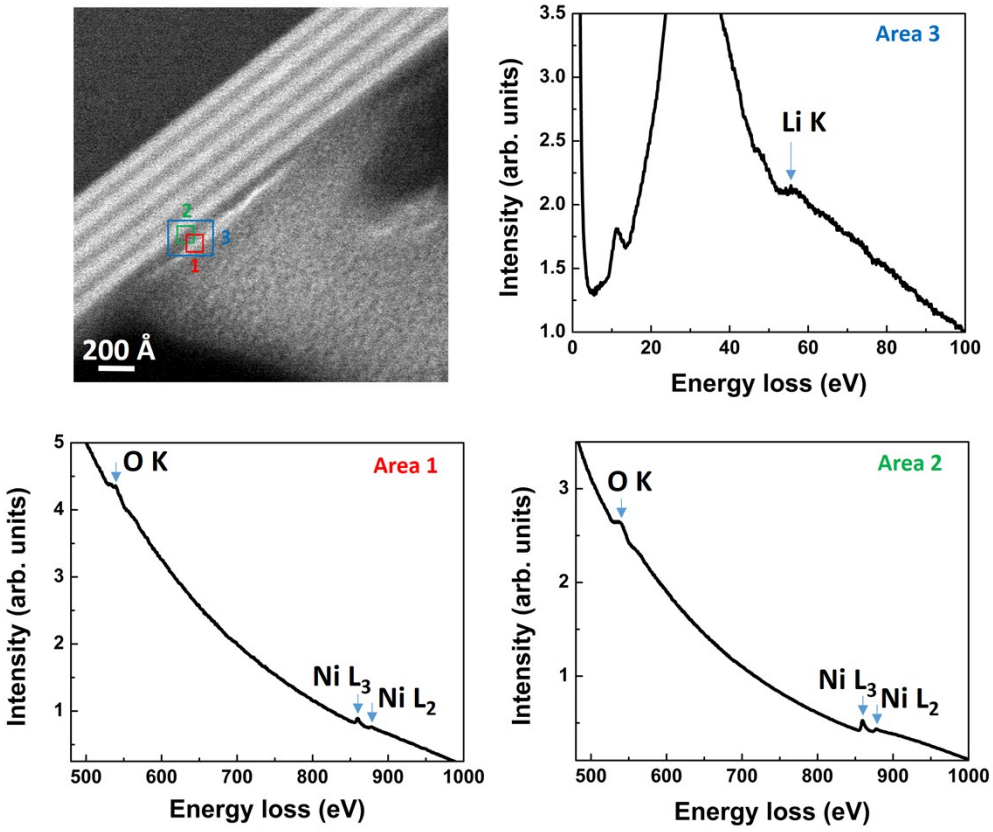

Fig. S1. EELS mapping of the reacted region, showing the signals of Li, Ni and O.

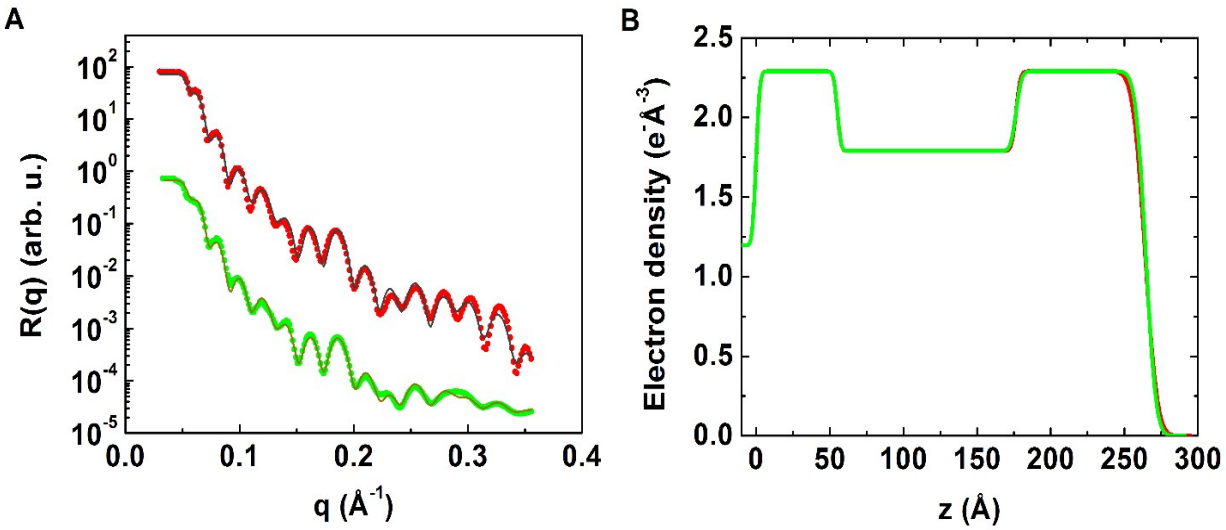

Fig. S2. A) The specular XRR (solid circles) and best fits (solid lines) for pristine trilayer Ni/NiO/Ni film with 89 Å thickness of the top Ni layer (blue) and for the same film after the first discharge cycle (green). The experimental and theoretical curves are shifted vertically for clarity.
B) The corresponding electron density profiles obtained from best fits of XRR data. For this case no significant change is observed.

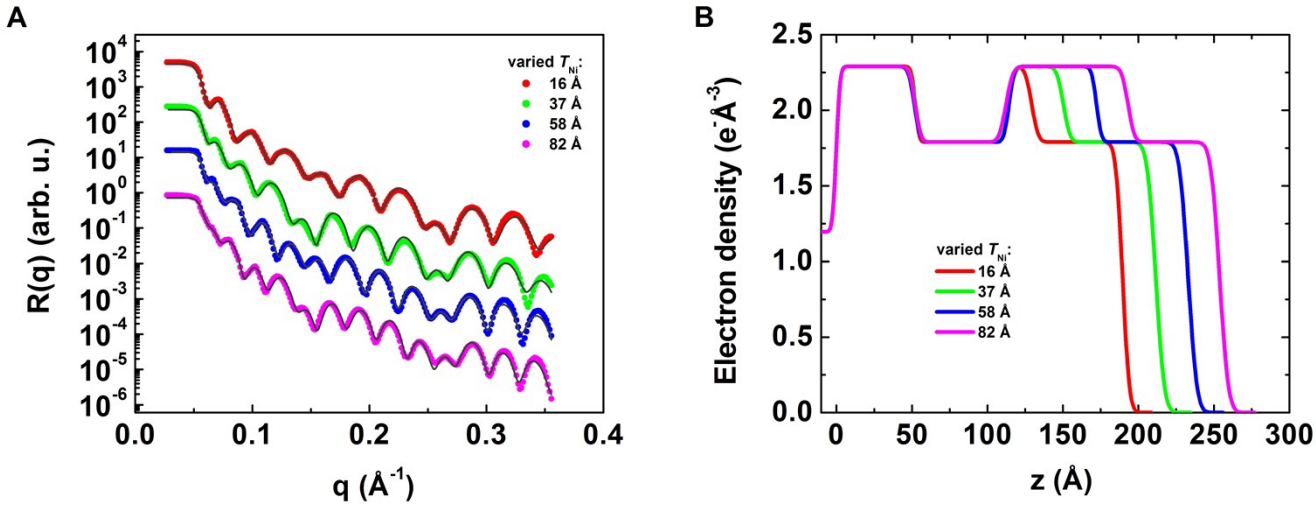

Fig. S3. A. The specular XRR (solid circles) and best fits (solid lines) for pristine 2-bilayer Ni/NiO structures with varied thickness of the Ni layer under the top NiO layer. The experimental and theoretical curves are shifted vertically for clarity. B. The corresponding electron density profiles obtained from best fits of XRR data.

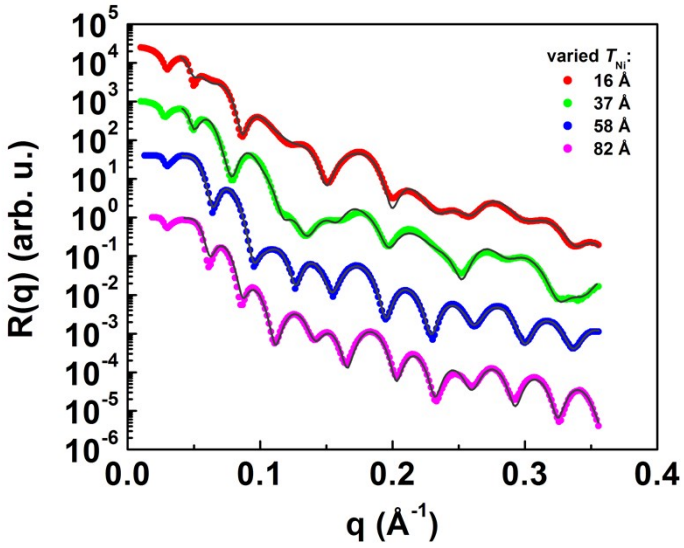

Fig. S4. The specular XRR data (solid circles) and best fits (solid lines) for lithiated 2-bilayer Ni/NiO films with varied thickness of the Ni layer under the top NiO layer. The experimental and theoretical curves are shifted vertically for clarity.

An additional Ni/NiO/Ni/NiO sample was lithiated and a second FIB cross-section TEM sample was analysed in order to confirm results seen in Fig. 9. The HAADF STEM image in Fig. S5 shows a similar layer morphology was found in the new sample post-lithiation. EELS line scan analysis of the oxygen K edge again revealed a strong peak in the fine structure at 538 eV, corresponding to NiO, and a strong shoulder at 535 eV indicating presence of Li_2O. Observing fine structure contributions from NiO for a second time suggests that the Ni formed from the

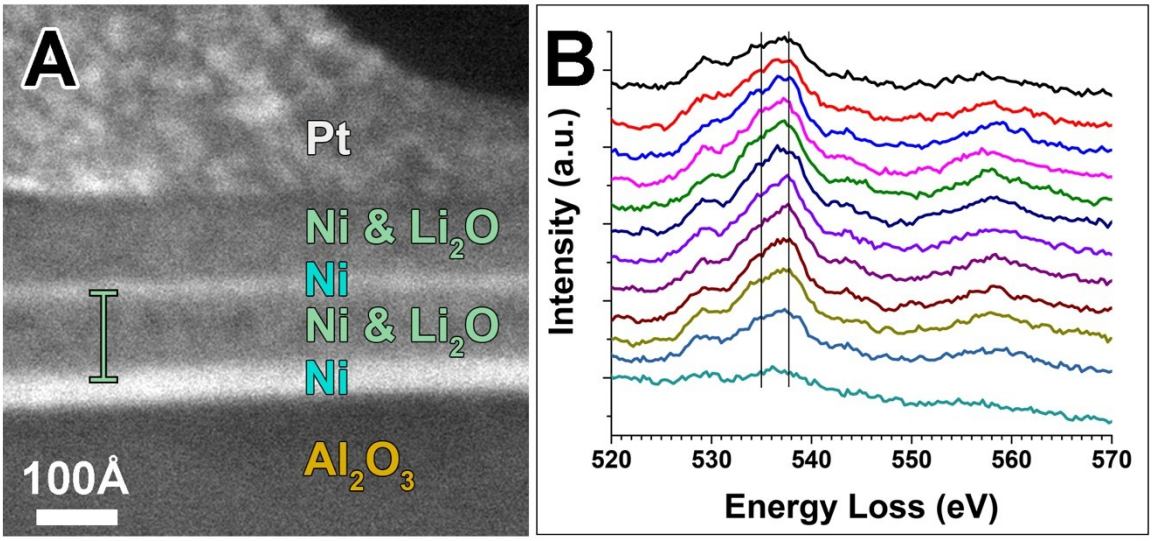

Fig. S5. EELS analysis of new multilayer sample. A) HAADF STEM image of 2-bilayer film with line scan area indicated. B) Oxygen K EELS line scan results with line markers indicating peak positions at 535 eV and 538 eV.

conversion reaction becomes oxidized during the short time it is exposed to atmosphere in the

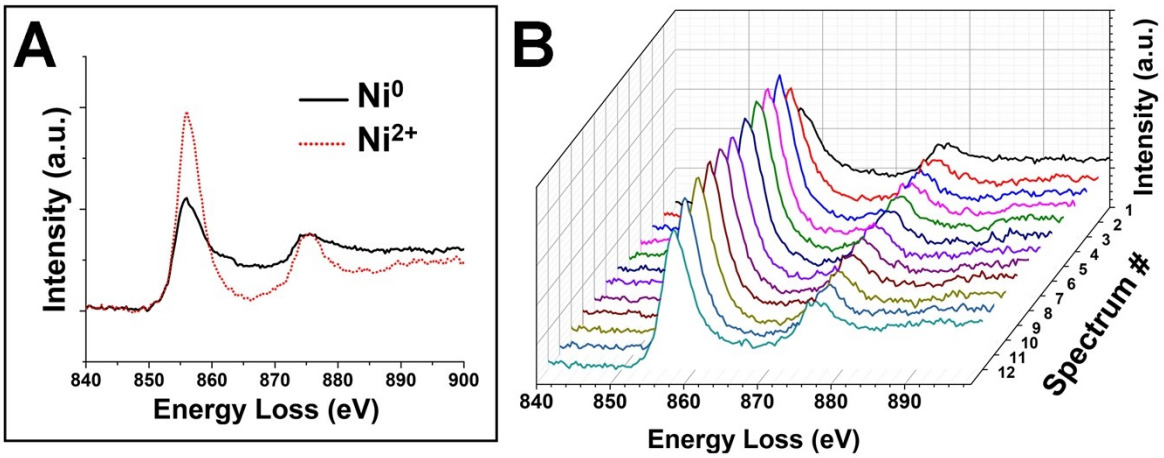

Fig. S6. EELS analysis of Ni $L_{3,2}$ edges. A) Fine structure comparison of Ni L_3 (855 eV) and L_2 (872 eV) edges in the metallic Ni and Ni^{2+} state. B) Line scan analysis of Ni $L_{3,2}$ edges.

sample preparation and handling process.

Analyzing the Ni $L_{3,2}$ edges from the EELS line scan also reveals the oxidation state of the Ni atoms throughout the layers in the multilayer structure. The Ni L_3 (855 eV) and L_2 (872 eV) edges directly correspond to electron transitions from 2*p* to available 3*d* states, and consequently demonstrate different edge fine structure and Ni L_3:L_2 "white line" intensity ratios which differentiate between metallic Ni and Ni atoms in a different oxidation state.[S1] EELS spectra of the Ni $L_{3,2}$ edges were collected from reference Ni and NiO samples, and the difference in Ni $L_{3,2}$ fine structure is seen in Fig. S6A, as the L_3 and L_2 edges have a more intense trailing edge for metallic Ni. Fig. S6B shows that only Spectrum 1 (black color) from Fig. S5 shows a fine structure corresponding to Ni^0, as that spectrum was collected from the upper Ni buffer layer. The remaining spectra collected from the line scan region of the lower Ni and Li_2O layer show fine structure corresponding to Ni^{2+} in NiO.

The white line ratios of the Ni L_3:L_2 edges were calculated for core-loss EELS spectra obtained from Ni and NiO standard samples in addition to spectra obtained from the bottom NiO layer (which underwent conversion into Ni and Li_2O) and the bottom Ni layer of the two different cross-sectional samples used in Fig 9 and Figs. S5 and S6. The ratios were calculated by removing the EELS background using a standard power-law fit and integrating the EELS

signal in the Ni L_3 (852 eV to 865 eV) and Ni L_2 (872 eV to 880 eV) region. The intensity ratios were calculated and presented in Table S2. This analysis shows that the Ni & Li_2O layers in both Fig. 9 and Fig. S5 have Ni L_3:L_2 ratios that correspond to the Ni^{2+} oxidation state, which agrees with the oxygen K edge analysis. The pure Ni buffer layer in both cases also has a Ni L_3:L_2 ratio that matches the Ni metal standard, indicated little-to-no oxidation of the buffer layer. This suggests that the Ni formed as the conversion reaction product is very susceptible to oxidation.

Table S2. Ni $L_{3,2}$ white line ratios for reference samples and experimental line scan data.

Sample	Ni L_3:L_2 Ratio
NiO Standard	1.84
Ni Standard	1.45
Ni & Li_2O Layer from Fig. 9	1.80
Ni Layer from Fig. 9	1.41
Ni & Li_2O Layer from Fig. S5	1.74
Ni Layer from Fig. S5	1.39

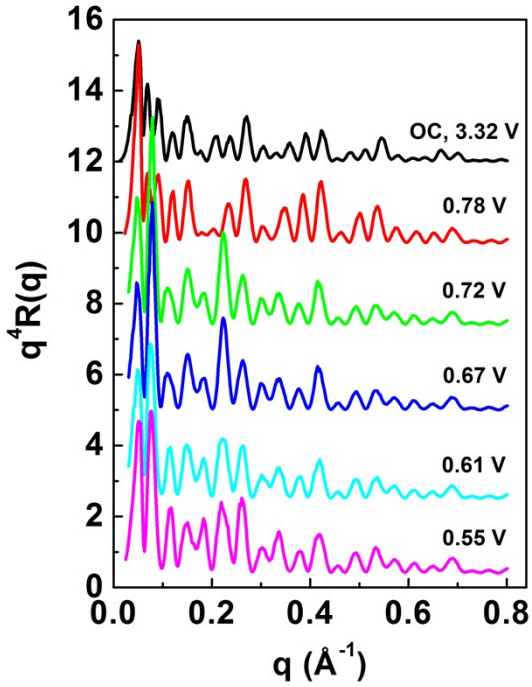

Fig. S7. The normalized in-operando X-ray reflectivity data for 2-bilayer Ni/NiO film during the first discharge (lithiation). To emphasize changes the reflectivity data, *R(q),* is normalized to the reflectivity from a single interface by being multiplied by q^4, where $q = (4\pi/\lambda)\sin\theta$ is X-ray momentum transfer along the surface normal. The curves are shifted vertically for clarity.

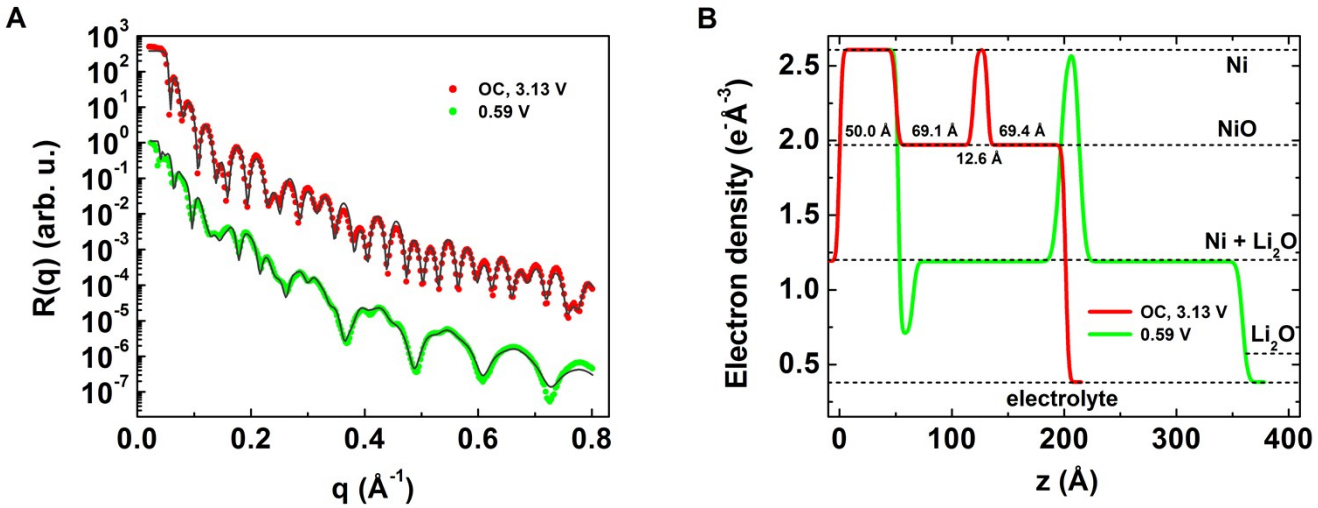

Fig. S8. A. The specular XRR (solid circles) and best fits (solid lines) for pristine 2-bilayer Ni/NiO film (red) and for the same film after the first discharge cycle (green). The experimental and theoretical curves are shifted vertically for clarity. B. The corresponding electron density profiles obtained from best fits of XRR data.

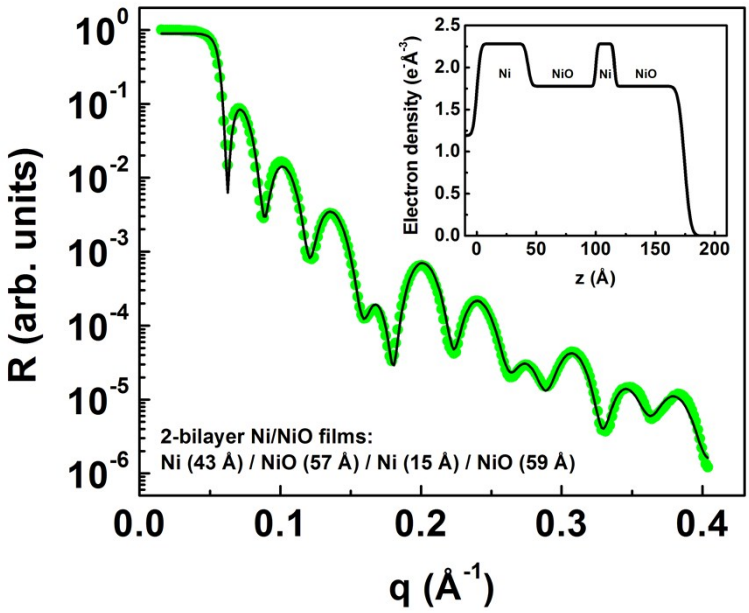

Fig. S9. Specular XRR data (solid circles) and best fit (solid line) for pristine 2-bilayer Ni/NiO film. Electron density profile obtained from best fit of the XRR data shown in the inset.

(S1) J. Graetz, C. C. Ahn, H. Ouyang, P. Rez, B. Fultz, White lines and D-band occupancy for the 3d transition-metal oxides and lithium transition-metal oxides, *Phys. Rev.* B, 2004, **69**(23), 235103 (6).